
Article:
Bala, A., Brown, J. R., Jenkins, D. G. orcid.org/0000-0001-9895-3341 et al. (1 more author) (2021) Operation of scintillators and SiPMs at high temperatures and their application for borehole logging. Nuclear Instruments and Methods in Physics Research, Section A: Accelerators, Spectrometers, Detectors and Associated Equipment. 165161. ISSN: 0168-9002

https://doi.org/10.1016/j.nima.2021.165161

Graphical Abstract

Operation of scintillators and SiPMs at high temperatures and their application for borehole logging

A. Bala, J.R. Brown, D.G. Jenkins, P. Joshi

Highlights

Operation of scintillators and SiPMs at high temperatures and their application for borehole logging

A. Bala, J.R. Brown, D.G. Jenkins, P. Joshi

- Research highlight 1
- Research highlight 2

Operation of scintillators and SiPMs at high temperatures and their application for borehole logging

A. Bala[a,b,*], J.R. Brown[a,**], D.G. Jenkins[a], P. Joshi[a]

[a] *Department of Physics, University of York, YO10 5DD, York, UK*
[b] *Department of Physics, Usmanu Danfodiyo University, P.M.B. 2346, Sokoto, Nigeria*

Abstract

Gamma-ray detection is extensively used in borehole logging — a technique widely employed in oil and gas, and mineral exploration. The workhorse of this detection application for many years has been traditional NaI(Tl) scintillators coupled to photo-multiplier tubes (PMTs) which can provide the performance and energy resolution required in this application. PMTs are a well proven technology which can operate in the high temperature conditions (typically of order 100°C) and pressures (10 MPa) encountered during logging activities. PMTs are, however, fragile in that they incorporate an evacuated tube. They also have a large form factor and require ancillary electronics such as a high-voltage supply meaning they occupy significant space within the borehole probe. It would be advantageous to have a compact replacement to allow additional instruments to be included within the borehole probe. Silicon photo-multipliers (SiPMs) are an attractive PMT replacement since they are robust, compact and operate at low voltage. However, SiPMs suffer from dark current which increases rapidly with temperature leading to increased noise and degraded energy resolution. We have evaluated CsI(Tl) scintillators coupled to standard 6×6 mm^2 SiPMs from Hamamatsu and SensL as a function of temperature. We have shown that these prototypes operate effectively up to a temperature of 80°C which could satisfy the requirements of some applications of borehole logging where the maximum temperature encountered is 75°C.

Keywords: Borehole logging, Inorganic scintillators, Silicon photomultipliers, Gamma-ray spectrometry

1. Introduction

Borehole logging is a technique used for studying geological formations as an aid to mineral (or oil and gas) exploration. Boreholes can be several hundred metres to a few kilometers deep, yet only ∼10 cm wide. At these depths, temperatures in excess of 100 °C and pressures of 10 MPa are typical, hence the instrumentation used in

*Corresponding author
**Corresponding author
Email addresses: aliyu.bala@york.ac.uk (A. Bala), jamie.brown@york.ac.uk (J.R. Brown)

borehole logging must be able to operate satisfactorily in this environment, meet the strict form-factor requirements, as well as be sufficiently rugged for use in a heavy industrial setting.

Gamma-ray detection is a common and useful aspect of borehole logging and is principally used in two applications:

1. γ-ray detection from naturally occurring sources in minerals. This application can be achieved with modest energy resolution since it relies on identifying the high-energy gamma peak from the decay of ^{40}K and a few gamma ray peaks from the progenies of Uranium and Thorium which are well separated.
2. Detection of Compton-scattered photons from a ^{137}Cs source to determine the density of materials surrounding the borehole probe. Here, energy resolution is not especially important but it is advantageous to be able to detect lower energy (< 100 keV) gamma rays to maximise efficiency and so that a ^{241}Am source (60 keV γ ray) can be employed for calibration.

The standard instrument used in both applications is a NaI(Tl) scintillator coupled to a photomultiplier tube (PMT). However, such devices, and their associated powersupplies, are rather bulky; a significant limitation given the very limited space available within a borehole probe. An alternative photosensor which is more compact would be of great interest in this application. An attractive replacement technology consists of silicon photomultipliers (SiPMs). These devices have been revolutionary in medical imaging applications [1, 2, 3, 4, 5] and are finding wider application in experimental nuclear physics as well as related societal applications. SiPMs are robust and have a small form factor and unlike PMTs, they do not need a high voltage. In recent years, a number of manufacturers have made advances in this technology resulting in higher gain, lower dark-count-rate (DCR), reduced cross-talk and after-pulsing, as well as reduced temperature sensitivity. These devices now present the possibility of creating a new generation of compact, low-voltage detectors for the borehole logging application.

In this work, we report on efforts to develop a SiPM-based detector suitable for replacing PMT-based gamma-ray detectors which was motivated by the needs of Robertson Geologging (RG), an international company active in the field of borehole logging who are based in North Wales. From their perspective, and with their years of experience in this field, they were strongly motivated to reduce the form factor of the radiation detectors especially gamma-ray detectors used in their borehole logging probes to permit more instruments to be accommodated in the probe at the same time. This would provide an important differentiator for them from competitor's offerings. Furthermore, for the market which they access which focuses on mineral exploration, an upper temperature rating of 75°C is compatible with the majority of applications which they support.

2. Choice of detector materials

Critical to this study is the choice of appropriate materials to form the prototype detector. Accordingly, we initially discuss the motivation for the selection of the scintillator crystals and SiPMs to be studied.

2.1. Choice of scintillator for high temperature operation

An ideal crystal should have good proportionality, strong scintillation emission and a suitable wavelength matching to typical SiPMs. $CeBr_3$ and $LaBr_3$:Ce are two options which have excellent proportionality and high light emission. Their cost as compared to the NaI:Tl makes them unsuitable for such an industrial application, particularly when energy resolution is not of utmost importance. A more practical choice are CsI:Tl and CsI:Na scintillators having peak emission wavelengths of 550 and 420 nm, respectively. They give very similar performance to NaI(Tl) and are only marginally more expensive, though with significantly longer decay times (1000 ns and 630 ns respectively, compared to 230 ns for NaI:Tl). However, they are a much better match to the performance of the SiPMs used in this work. Moreover, since they are only slightly hygroscopic, it is possible to dispense with canning, optical windows etc. and further save space.

As the detectors are to be operated at elevated temperature, the change in their light output as a function of temperature becomes a relevant consideration. If such crystals become brighter at the temperatures considered in this application then the improved photon statistics may at least partially offset the degradation of the SiPM performance at elevated temperature — an issue to be discussed in more detail below. Some authors have reported an increasing light output for CsI:Na[6, 7] peaking at ~80 °C. This would be of particular interest for the borehole logging application as 80 °C is within the typical operating temperature range, however it should be noted that the data cited are at odds with contemporary data sheets from Saint Gobain Crystals which indicate that both CsI:Tl and CsI:Na exhibit maximum light output at ~30 °C [8]. These considerations motivated the choice of CsI:Tl and CsI:Na as the crystals to be investigated in this study.

2.2. Choice of silicon photomultiplier

Silicon photomultipliers has spawned a number of new manufacturers, namely KeteK, AdvanSiD, First Sensor and Excelitas, in addition to the more established Hamamatsu and SensL. Compared to photodiodes and avalanche photodiodes (APDs), SiPM exhibit less temperature sensitivity, they are far from immune to temperature effects.The breakdown voltage of SiPM increases with temperature. Constant bias voltage manifests in peak height reduction due to the reduction in over-voltage (i.e. $V_{over} = V_{bias} - V_{breakdown}$) which leads to a reduction in gain with temperature. Small temperature changes results in photopeak broadening, leading to poor energy resolution. Peak shift will be

observed for large temperature changes, adjusting the bias voltage will mitigate this effect. Additionally, dark-count rate (DCR) increases with temperature as characterised by the rule of thumb: *dark-count rate roughly doubles for every 10°C increase*, i.e. $R(T) = R_0 \cdot 2^{(T-T_0)/10}$, where R is the dark-count rate at temperature T, and R_0 is the dark-count rate at temperature T_0.

In this study we focus on SiPMs from SensL and Hamamatsu, specifically SensL J-series and Hamamatsu S14160 (see table 1), principally due to their maximum operating temperatures of 85 °C which is significantly higher than other manufacturers at the time of evaluation. Both manufacturers refer to reflow soldering conditions exceeding 200 °C, however this is very short time process compared to logging time, so it worth investigating the maximum temperature both SiPMs can be subjected to without permanent degradation of performance. A recent publication [9] performed a comparison of SensL J-series and and an older generation of Hamamatsu SiPMs (S12642-0404PA) coupled to various scintillators including CsI:Tl and found very similar performance in terms of energy resolution, despite a number of different properties, e.g. breakdown voltage, micro-cell size, and photo-detection efficiency. However, the SensL device was found to be less sensitive to temperature and bias changes, and exhibited superior linearity due to the larger number of micro-cells.

Table 1: Characteristics of the SensL J-series and Hamamatsu S14160 SiPMs.

Characteristics	Hamamatsu	SensL
Technology	HWB (Hole Wire Bonding)	TSV (Through Silicon Via)
SiPM Type	S14160-6050HS	J-series
Effective area	6.0×6.0 mm^2	6.07×6.07 mm^2
Number of microcells	14,331	22,292
Breakdown voltage	37.0 V	24.5 V
Recommended overvoltage	2.7 V	2.5 V
Temperature coefficient	34 mV/°C	21.5 mV/°C
Gain	2.5×10^6	2.8×10^6
Crosstalk probability	7 %	8 %
Operating temperature	-40 to 85 °C	-40 to 85 °C

3. Results

3.1. Light output of CsI:Tl and CsI:Na as a function of temperature

Due to the confusion in the available literature on their light output as a function of temperature, the relative light output from CsI:Na and CsI:Tl crystals was investigated in the range 20-80 °C. Both crystals were 1" × 1" cylinders supplied by Hilger Crystals, wrapped with reflective wrapping and packaged within aluminium cans with optical

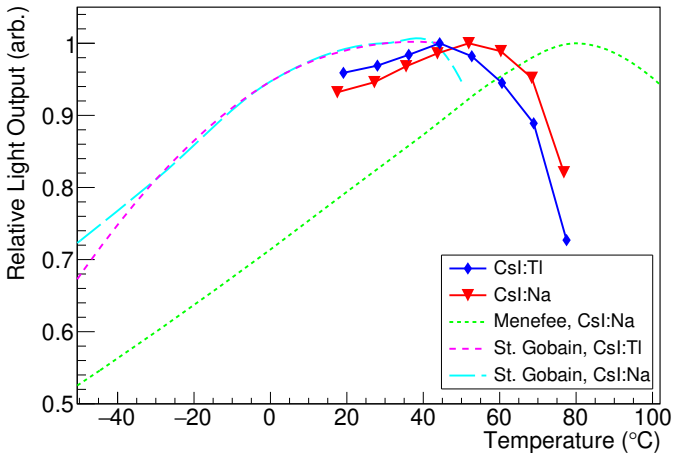

Figure 1: Relative light output as a function of temperature for CsI:Tl and CsI:Na crystals, as measured in this work, and compared to that reported in references [7] and [8].

windows on one face. Though this canning was not strictly necessary for CsI:Tl due to its minimal hygroscopicity, getting identically packaged crystals allows for a direct comparison of the two materials.

Measurements were performed by coupling each of the crystals to a 2×2 array of Hamamatsu SiPMs (S13361-6050NE-02). The SiPMs were biased to a nominal voltage of 57 V at room temperature and varied with temperature so as to maintain a constant over-voltage and hence gain, based on the manufacturers specifications (54 mV/°C). The peak position of the 662 keV photopeak was measured at temperatures ranging from 20—80°C and used as a measure of light output. It is expected that the linear relationship between breakdown voltage and temperature may not hold at the highest temperatures encountered in this experiment, however as both scintillators were treated the same way, any change in SiPM gain will affect both measurements identically, hence will not influence the results reported here. A short shaping time was used so as to achieve the best possible performance at high temperature (see section 3.2).

The result of this investigation can be seen in figure 1, along with relative light outputs taken from [7] and [8]. In each case the light output has been normalised to the maximum to aid comparison. The results obtained here indicate that light output peaks at approximately 44 °C and 52 °C for CsI:Tl and CsI:Na respectively, as opposed to ~80 °C as reported by Menefee et al. [7] or ~30 °C as reported by Saint Gobain [8]. The result presented here is based on a single sample, and is not intended to refute the above values quoted by the manufacturer.

These measurements were performed by increasing the temperature of the chamber in stages and waiting until the temperature measured on the surface of the crystal became stable. It is possible that the wait time was not sufficient to allow the centre of the crystals to reach the measured temperature, in which case the temperatures reported in figure 1 would be artificially high. This effect could partially explain the discrepancy with the Saint Gobain data, however the

Menefee et al. [7] result, indicating peak light output at ~80 °C, is firmly refuted. Based on this result, (and bearing in mind that the absolute light output from CsI:Na is lower than that of CsI:Tl) we find no reason to favour CsI:Na over CsI:Tl for high temperature applications. Accordingly, unless otherwise stated, CsI:Tl is used throughout the remainder of this work.

It should be noted that an additional bare CsI:Tl crystal of the same dimensions was wrapped with PTFE and tested at room temperature. The light collected from this crystal was approximately twice that of the canned crystal. It is not known whether this difference was due to the quality of the wrapping or a result of light losses in the optical window. Nevertheless, it highlights the importance of careful wrapping and coupling of scintillator crystals, as discussed further in [10].

3.2. Energy resolution vs shaping time at room temperature and high temperature

In order to evaluate the performance of prototype detectors coupiling CsI:Tl crystals to SiPMs, optimum operating parameters must be found, specifically bias and shaping time. The detector is ideally required to measure down to 60 keV so that it can be calibrated using a ^{241}Am source which is the standard procedure followed by Robertson Geologging, hence there is a risk of the noise floor increasing beyond this signal level. As such, signal-to-noise ratio is an important figure-of-merit. Accurate measurement of the noise level is not straightforward hence the FWHM of the 662 keV photopeak is used as a proxy for this, despite energy resolution not being of critical importance for this application. FWHM at 662 keV is calculated following a quadratic energy calibration based on fits to peaks from 121 to 1408 keV from a ^{152}Eu source, in order to correct for any non-linearity.

Prototype detector assemblies were produced coupling a 7×7×25 mm^3 CsI:Tl crystal to either a 6×6 mm^2 SensL J-series SiPM or a 6×6 mm^2 Hamamatsu S14160-6050HS series SiPM. The size of the crystal was chosen to match the dimensions of the SiPMs. In a real application a significantly larger, more efficient crystal would be required to measure the activities of interest. The scintillator crystals were wrapped with a minimum of eight layers of 0.2 mm PTFE tape and coupled to the photosensors using silicone-based optical grease (EJ-550). The nominal biases applied to the SensL J-series SiPM and Hamamatsu S14160-6050HS series SiPM were 29 V and 41 V, respectively. Detector readout was performed using an Ortec 571 shaping amplifier (with shaping times ranging from 0.5 to 10 μs) and a multi-channel analyser (Ortec EASY-MCA). Gamma-ray spectra were acquired using ^{137}Cs and ^{152}Eu sources to allow for energy calibration, linearity correction and measurement of energy resolution. Measurements were performed within a temperature controlled chamber, with a thermocouple placed in close proximity to the SiPM board to allow monitoring of the temperature. A schematic of this set up is shown in figure 2.

In figure 3, the linearity-corrected FWHM of the 662 keV photopeak is plotted as a function of shaping time. For all the measurements, the best resolution is observed at longer shaping times, which can be understood due to the

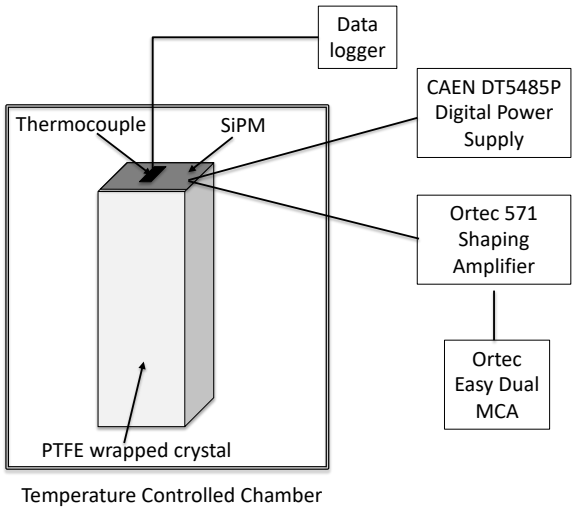

Figure 2: Schematic of the experimental setup used throughout this work.

long decay time of CsI:Tl. However, as can be seen from figure 4, when these measurements are repeated at high temperature (70°C) this situation changes dramatically. This can be explained when we consider that the noise is the sum of series and parallel noise. The low temperature curves are consistent with a standard noise model with negligible current noise (the curve forms a shallow minimum, not reached within this range of shaping times). When the temperature is increased the dark-count rate increases, which can be treated as a source of current noise, thus is more significant for longer shaping times [11]. We should also note here that the decay time of CsI:Tl is known to reduce with increasing temperature [12], which may contribute to the shift to lower optimal shaping time at higher temperatures. Nevertheless, it is clear from figure 4 that shorter shaping times (2 μs or less) should be used at high temperature so as to minimise the contribution of this increased parallel noise. Accordingly, 2 μs shaping time is used as the optimum setting at high temperature with the standard electronics setup for the rest of this work.

3.3. Energy resolution vs bias at room temperature and high temperature

Figures 5 and 6 show the bias optimisation of 6×6 mm^2 Hamamatsu S14160-6050HS and SensL J-series SiPMs respectively at room temperature and high temperature. The optimum operating voltages at room temperature are found to be 27.8 V and 41.0 V for SensL and Hamamatsu SiPMs: the corresponding ^{137}Cs and ^{152}Eu spectra can be seen in figures 7 and 8.

As was found for the shaping time, optimum operating conditions at high temperature differ significantly from

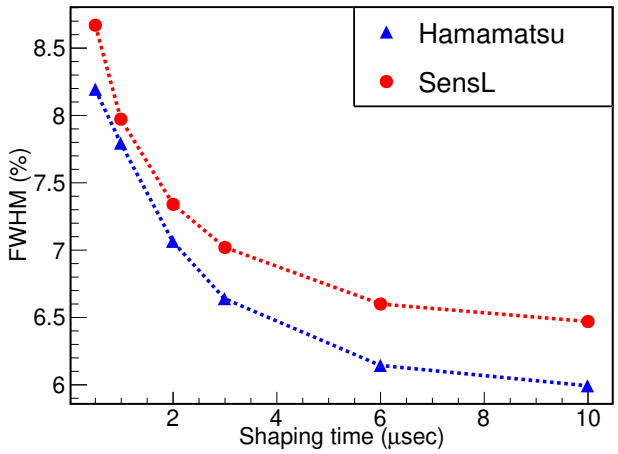

Figure 3: Linearity corrected energy resolution (at 662keV) as a function of shaping time for 6×6 mm^2 SensL J-series SiPM (red) and Hamamatsu S14160-6050HS (blue) each coupled to a 7×7×25 mm^3 CsI:Tl and operated at 29 V and 41 V respectively at room temperature.

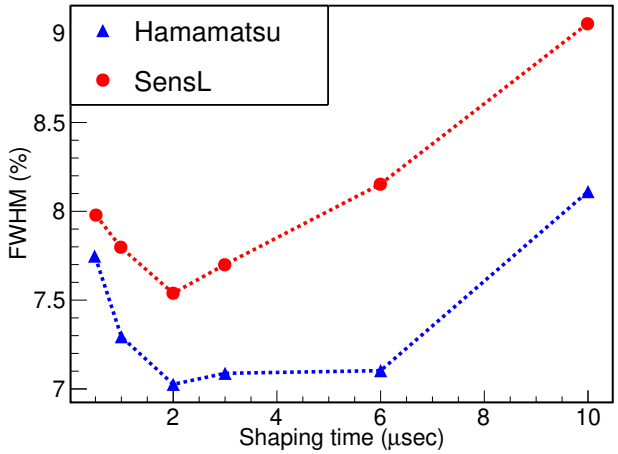

Figure 4: Energy resolution as a function of shaping time for SensL J-series (red) and Hamamatsu S14160-6050HS (blue) SiPM at a bias voltage of 29 V and 41 V respectively, with temperature measured at 70°C.

those found at room temperature. This can be explained via similar arguments to those used in section 3.2. As the dark count rate (i.e. noise) increases exponentially with temperature, a bias voltage chosen to maximise the signal-to-noise ratio at room temperature will not be optimal at higher temperatures.

A summary of the results obtained in terms of energy resolution and the optimised detector parameters such as bias voltage and shaping time is presented in table 2.

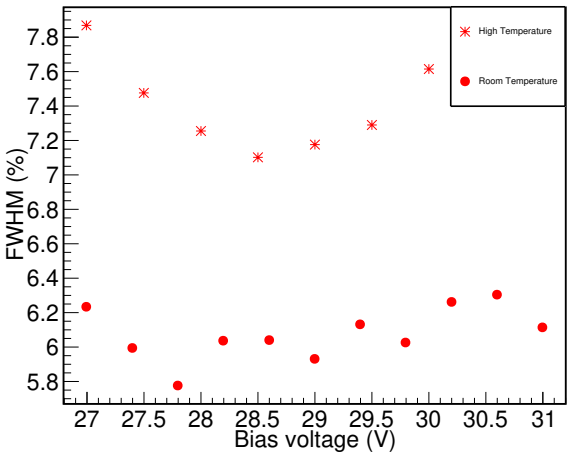

Figure 5: Linearity corrected energy resolution (at 662keV) as a function of bias voltage for 6×6 mm^2 SensL J-series SiPM coupled to a 7×7×25 mm^3 CsI:Tl, at room and high temperature (high temperature chamber set to 70 °C)

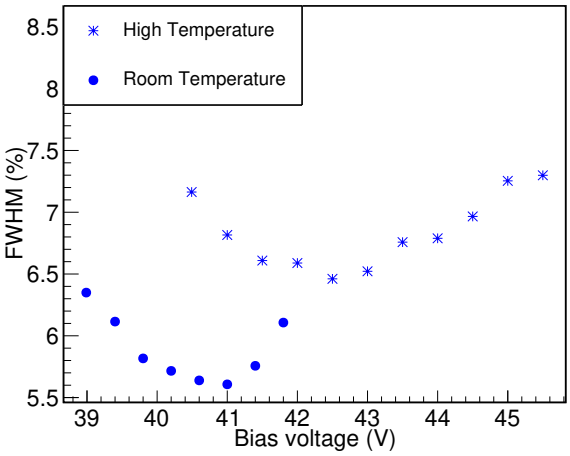

Figure 6: Linearity corrected energy resolution (at 662keV) as a function of bias voltage for 6 ×6 mm^2 Hamamatsu S14160-6050HS SiPM coupled to a 7×7×25 mm^3 CsI:Tl, at room and high temperature (high temperature chamber set to 70 °C)

3.4. Temperature dependent gain stabilisation

In order to operate an SiPM over the large range of temperatures encountered during a well-logging measurement the bias must be adjusted to maintain a constant gain. This method is essential as going to higher temperatures will cause the breakdown voltage to increase beyond the nominal room temperature bias setting, leading to a complete loss of signal. Using the optimum settings found for our high temperature measurements, spectra were obtained at 80°C with a ^{137}Cs source and the centroid of the 662 keV peak was noted. Spectra were then taken over a range of temperatures from 20 to 80°C, at each point adjusting the bias to match the peak position at 80°C. These spectra are shown in figures 9 and 10. The increasing noise is evident on the left-hand-side of these spectra, with the 32 keV

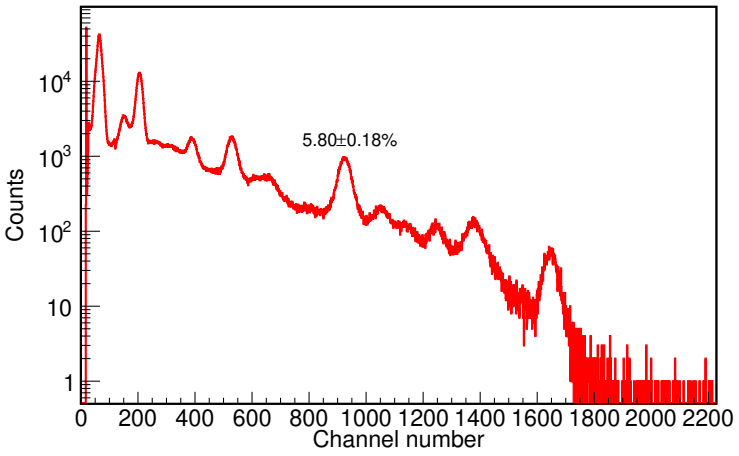

Figure 7: Energy spectrum for ^{137}Cs and ^{152}Eu radioactive sources, measured with a 6×6 mm^2 SensL SiPM coupled to a 7×7×25 mm^3 CsI:Tl at room temperature using 10 μs shaping time and a bias voltage of 27.8 V. The FWHM of the 662-keV peak was 5.80(18) %.

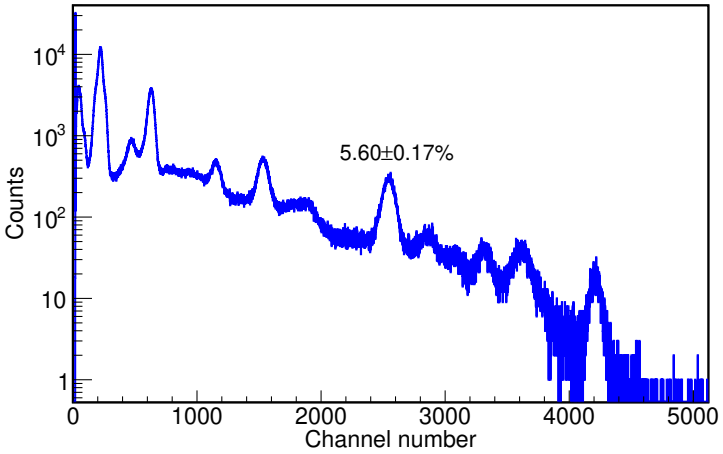

Figure 8: Energy spectrum for ^{137}Cs and ^{152}Eu radioactive sources measured with a 6×6 mm^2 Hamamatsu SiPM coupled to a 7×7×25 mm^3 CsI:Tl at room temperature using 10 μs shaping time and a bias voltage of 41 V. The FWHM of the 662-keV peak was 5.60(17) %.

X-ray becoming obscured at the highest temperatures. In the case of the SensL SiPM at 80°C, this noise is sufficient to conflict with the requirement to detect gamma rays below 100 keV.

The bias voltages required to maintain the 662-keV peak position are plotted as a function of temperature in figures 11 and 12 for the Hamamatsu and SensL SiPM respectively. From linear fits to these data we find average temperature compensation coefficients of 38.6 mV/°C and 27.4 mV/°C for the Hamamatsu and SensL SiPMs respectively, somewhat different to the values of 34 mV/°C and 21.5 mV/°C quoted in the respective data sheets as can be seen in table 1 above. Furthermore, it is clear from the fits presented in figures 11 and 12 that a purely linear temperature compensation is not sufficient to stabilise the peak position over the large temperature range investigated here. Quadratic fits

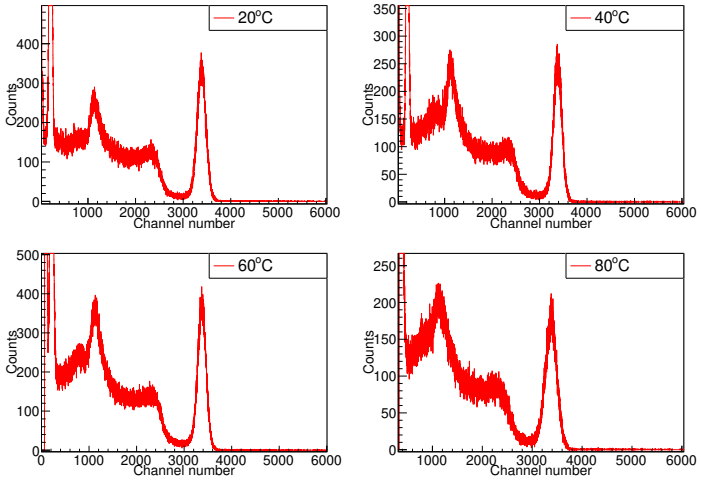

Figure 9: Spectra obtained with the SensL SiPM at 20°C (top left panel), 40°C (top right panel), 60°C (bottom left panel) and 80°C (bottom right panel), manually adjusting the bias voltage to achieve the same 662-keV peak position (see text).

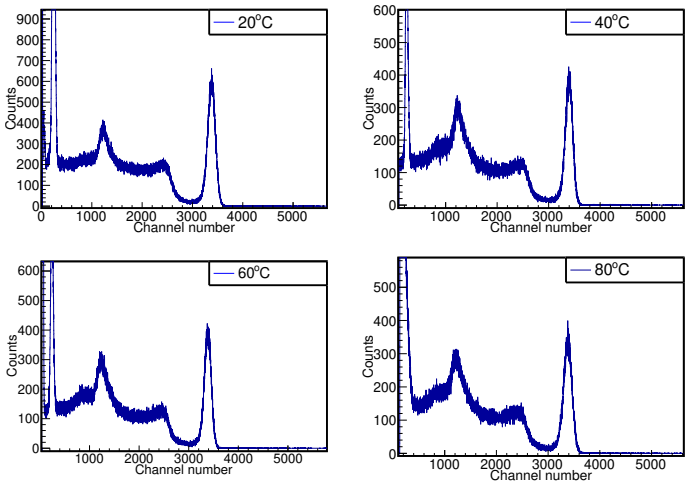

Figure 10: Spectra obtained with the Hamamatsu SiPM at 20°C (top left panel), 40°C (top right panel), 60°C (bottom left panel) and 80°C (bottom right panel), manually adjusting the bias voltage to achieve the same 662-keV peak position (see text).

Table 2: Optimum characteristics of the SiPMs tested.

Characteristics	6×6 mm^2 Ham.	6×6 mm^2 SensL
Optimum shaping time (22°C)	10 μsec	10 μsec
Optimum shaping time (70°C)	2 μsec	2 μsec
Optimum bias voltage (22°C)	41.0 V	27.8 V
Optimum bias voltage (70°C)	42.5 V	28.5 V
Breakdown voltage	38.2 V	25.3 V
Energy Resolution (662 keV) at (22°C)	5.6%	5.8%
Energy Resolution (662 keV) at (70°C)	6.5%	7.1%

to these data were also performed and found to better reproduce the observed behaviour.

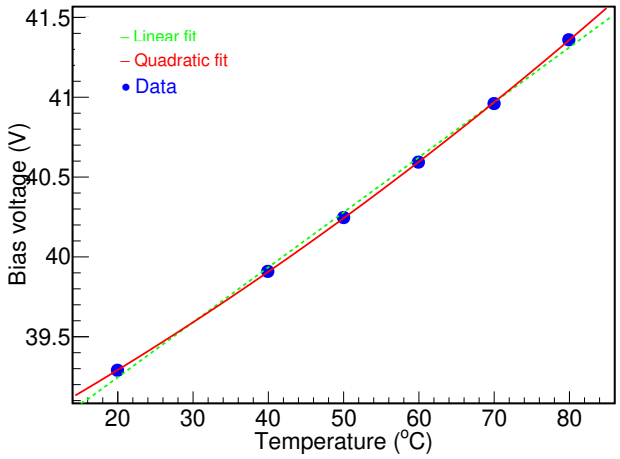

Figure 11: Bias required to maintain a constant 662-keV peak position, as a function of temperature for Hamamatsu SiPM, along with linear and quadratic fits to the data.

In figure 13, we present the energy resolution for the (linearity corrected) 662 keV peak, obtained from these spectra. Unsurprisingly, because the system has been optimised for the high temperature case, the resolution achieved at low temperatures is significantly worse than was achieved in sections 3.2 and 3.3. Furthermore, although there is some variation of FWHM across the temperature range and, notably, the strong degradation of performance of the SensL SiPM at the highest temperature considered, the variation is not large enough to conflict with the modest resolution requirements of this application.

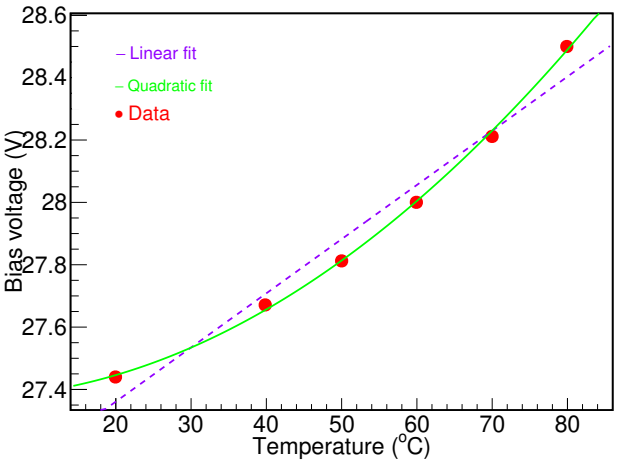

Figure 12: Bias required to maintain a constant 662-keV peak position, as a function of temperature for SensL SiPM, along with linear and quadratic fits to the data.

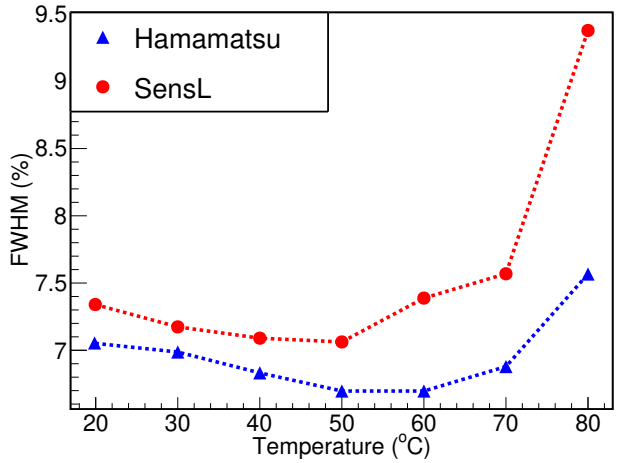

Figure 13: Corrected energy resolution (at 662keV) as a function of temperature for 7×7×25 mm^3 CsI:Tl coupled to a 6×6 mm^2 Hamamatsu S14160-6050HS (blue) and SensL J series SiPMs (red) respectively, with varying bias voltage.

4. Temperature compensation bias supply

In this section and in the continued project, our focus is to produce a bespoke, miniaturised temperature-compensated bias supply that would be appropriate to operate in the conditions experienced in borehole logging. This supply may well be different to what is available off the shelf. The device is controlled by an Arduino board, allowing it to be programmed to deliver the output voltage as any function of temperature. A circuit diagram of the device is shown in figure 14. The board interfaces with a daughter board which holds the SiPM array and a digital temperature sensing chip (ADT7310).

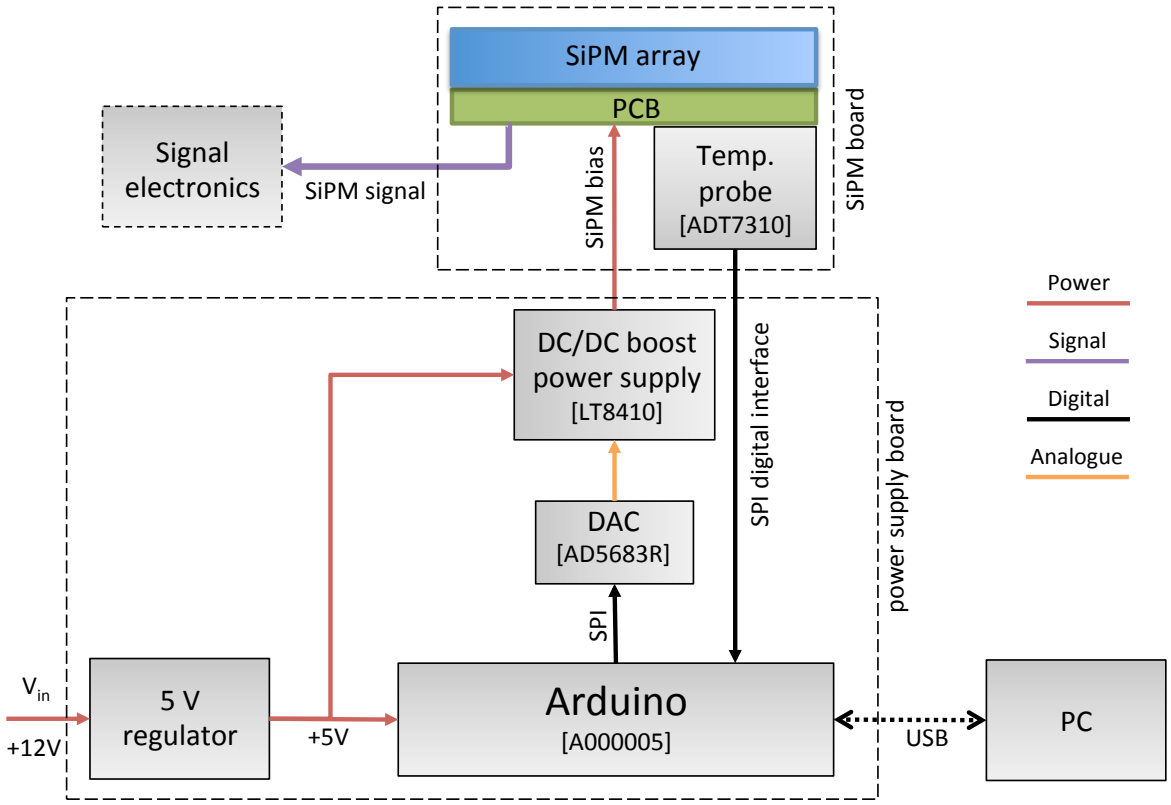

Figure 14: Schematic diagram of the temperature compensation power supply. The PC connection is only required whilst programming the supply.

The performance of the power-supply module can be seen in figure 15, for a 2×2 SensL J-series array, characterised from 20 to 80°C as described in section 3.4. Using a quadratic temperature compensation function, the module successfully stabilises the gain maintaining the peak position throughout the energy range up to 70°C. Beyond this temperature, the module was unable to deliver enough current to maintain the desired over-bias for this 2×2 array. A new version of the power-supply is being developed which will be able to deliver more current to allow gain stabilisation at higher temperature, as well as achieve higher bias voltages making it compatible with SiPMs from

other manufacturers such as Hamamatsu.

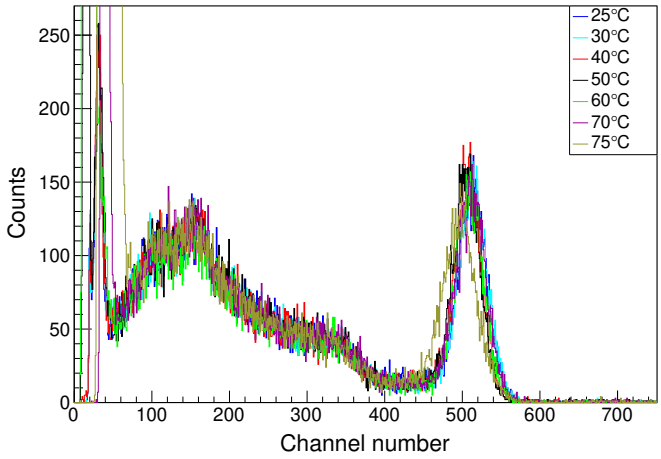

Figure 15: ^{137}Cs spectra obtained with a range of temperatures, with a variable bias supplied by a temperature compensation power-supply module.

5. Conclusion

Temperature sensitivity is a key parameter for photo-sensors which might be coupled to scintillators and used in borehole logging. We have demonstrated the suitability of modern SiPM technology to replace the current standard PMT based instruments, providing benefits such as reductions in form factor and low voltage requirements. The characterisation carried out provides an indication of the performance that can be expected from an SiPM based detector system for a well-logging application and it is seen to be comparable to that from a standard NaI:Tl plus PMT solution. While we have demonstrated that both the SensL and Hamamatsu SiPMs are suitable in such an application, the superior energy resolution, smaller temperature dependence, and crucially, the lower noise at high temperatures, would make the Hamamatsu SiPM the preferred choice for this challenging environment. Furthermore, we have presented results on the performance of a prototype temperature compensating SiPM power supply suitable for use in such an application.

6. Acknowledgement

Sincere gratitude to Petroleum Technology Development Fund (PTDF) who fully funded this work. We acknowledge the support of Robertson Geologging, especially Paul Worthington who provided information on the context of gamma-ray detection in borehole logging. Aliyu Bala also acknowledges Robertson Geologging for hosting him at their headquarters for two weeks during 2018.

References

[1] M. G. Bisogni, A. Del Guerra, N. Belcari, Medical applications of silicon photomultipliers, Nuclear Instruments and Methods in Physics Research Section A: Accelerators, Spectrometers, Detectors and Associated Equipment 926 (2019) 118 – 128.

[2] G. Llosá, SiPM-based compton cameras, Nuclear Instruments and Methods in Physics Research 926 (2019) 148 – 152.

[3] H. Park, J. S. Lee, Highly multiplexed SiPM signal readout for brain-dedicated TOF-DOI PET detectors, Physica Medica 68 (2019) 117 – 123.

[4] J. Jeon, H. Lee, J. Lee, Fabrication and testing of a 1024-pixel SiPM camera, Nuclear Instruments and Methods in Physics Research 958 (2020) 162839.

[5] K. Shimazoe, M. Yoshino, Y. Ohshima, M. Uenomachi, K. Oogane, T. Orita, H. Takahashi, K. Kamada, A. Yoshikawa, M. Takahashi, Development of simultaneous pet and compton imaging using GAGG-SiPM based pixel detectors, Nuclear Instruments and Methods in Physics Research Section A: Accelerators, Spectrometers, Detectors and Associated Equipment 954 (2020) 161499.

[6] Nakayama, M and Ando, N and Hirai, J and Nishimura, H, Scintillation activated by nanoparticle formation in CsI:Na thin films, Journal of Luminescence 108 (1-4) (2004) 359–363.

[7] Menefee, J and Cho, Y and Swinehart, C, Sodium Activated Cesium Iodide as a Gamma Ray and Charged Particle Detector, IEEE Transactions on Nuclear Science 14 (1) (1967) 464–467.

[8] Gobain, Saint, CsI(Tl), CsI(Na) Cesium Iodide Scintillation Material (Aug. 2016).

[9] Grodzicka-Kobylka, M and Szczesniak, T and Moszynski, M, Comparison of SensL and Hamamatsu 4×4 channel SiPM arrays in gamma spectrometry with scintillators, Nuclear Inst. and Methods in Physics Research, A 856 (2017) 53–64.

[10] Brown, J R and Paschalis, S and Jenkins, D and Joshi, P and Marsden, E and Bell, A and Mullins, J, Performance of advanced scintillator materials : A comparison of coupling and wrapping techniques with PMTs and SiPMs (in preparation).

[11] G. F. Knoll, Radiation Detection and Measurement, Wiley, New York, NY, 2010.

[12] J. D. Valentine, W. W. Moses, S. E. Derenzo, D. K. Wehe, G. F. Knoll, Temperature dependence of CsI(Tl) gamma-ray excited scintillation characteristics, Nuclear Inst. and Methods in Physics Research, A 325 (1-2) (1993) 147–157.